

## **Surface-consistent Gabor deconvolution**

Carlos A. Montaña, Gary F. Margrave and David C. Henley

### **ABSTRACT**

Anelastic attenuation of seismic energy is considered to be a minimum phase process. Gabor deconvolution aims at the simultaneous elimination of both the attenuation effects and the source wavelet, which in the case of explosive sources is also considered to be minimum phase. In the absence of an accurate estimation of  $Q$ , the phase component of the Gabor deconvolution operator is designed with the help of the digital Hilbert transform. The digital Hilbert transform, however, may suffer serious distortions when the seismic trace presents a poor signal to noise ratio. As redundancy is the best protection against the harmful effects of random noise, a more robust implementation of the Gabor deconvolution method can be obtained through the use of the surface consistency assumption. In this work, the nonstationary convolutional model for the seismic trace is slightly modified and converted into a surface-consistent model. The resulting surface-consistent Gabor deconvolution method is less sensitive to the presence of random and coherent noise, and surface consistent variations in the near-surface effects.

### **INTRODUCTION**

Gabor deconvolution, in its single channel version, has been tested on real data successfully several times. Margrave et al. (2004) reported extensively one of tests run by Sensor geophysics, and Perz et al. (2005) showed the results of processing 5 seismic lines using Gabor deconvolution. In both cases the Gabor results were compared with the results obtained using conventional processing in which surface consistent deconvolution is combined with time variant spectral whitening. In none of the tests could a clear advantage of one of the methods over the other be observed.

Additionally to the 5 real seismic lines, Perz et al. (2005) ran an experiment on a synthetic dataset, with the objective of testing the performance of surface-consistent algorithms. This dataset, described in detail below, represents a tough test for any deconvolution and/or attenuation compensation algorithm. The dataset presents a challenge due to the combination of three elements: 1) strong anelastic attenuation; 2) poor signal to noise ratio in a significant portion of the data; and 3) surface-consistent incorporation of source and receiver minimum phase wavelets. The results obtained after running single channel Gabor deconvolution on this dataset uncovered a weakness in the single trace Gabor algorithm, which in the presence of too small signal to noise ratio in the data, could potentially introduce undesirable artefacts. The problem is related to the use of the Hilbert transform in the computation of the minimum phase component of the Gabor deconvolution operator.

The use of the Hilbert transform in the Gabor deconvolution algorithm is a consequence of the physical mathematical model on which the method is based. Gabor deconvolution is in essence a nonstationary extension of the Wiener deconvolution method. This extension is made possible with the help of 3 theoretical elements: the

constant Q theory for attenuation (Kjartanson, 1979), the nonstationary convolutional model (Margrave, 1998) and the Gabor transform (e.g. Merlins, 1999). In the constant Q theory for attenuation, in which Q is considered independent of frequency, the concept of minimum phase arises as a consequence of linearity, causality and dispersion (Futterman, 1962). Anelastic attenuation is thus considered a minimum phase process in the constant Q theory, and therefore the operators designed to compensate for its effects are also minimum phase. The use of the digital Hilbert transform in the design of the Gabor deconvolution operator is based on the following important result from mathematics: in a minimum phase function, the phase spectrum is equal to the Hilbert transform of the logarithm of the amplitude spectrum.

Although the constant Q theory for attenuation finds an analytical expression to compute the Hilbert transform of the attenuation function (e.g. Aki and Richards, 2001), the explicit dependence of this analytical expression on Q makes it inappropriate for the cases when either a poor estimation of Q, or no estimation at all is available. In these cases the estimation of the phase through the Hilbert transform of the logarithm of the amplitude spectrum seems to be a more suitable alternative.

One of the drawbacks of using the digital implementation of the Hilbert transform to compute the phase is its high sensitivity to noise. The digital Hilbert transform is a discrete implementation of the mathematical definition of the Hilbert transform given for continuous functions. The mathematical definition involves an integral over all the frequencies with the consequence that the presence of noise at any the frequency will affect the estimation of the phase at all frequencies. This is the reason that the use of the Hilbert transform on data with low signal to noise ratio leads to poor results in the computation of the phase. One of the potential solutions to this problem is the application of the surface consistency assumption, thus taking advantage of the redundancy of the seismic data to attenuate the distorting effects of noise in the design of the deconvolution operators. An alternative solution called ‘Ensemble based deconvolution’ is presented by Henley et al. (2006), in a different paper of this report.

The performance of a minimum phase, surface-consistent Gabor deconvolution method in the presence of high levels of random noise is examined in this paper. A synthetic seismic dataset, courtesy of DIVESTCO, is used to illustrate the problem and its surface-consistent solution.

## **THEORY**

### **The theoretical fundamentals of Gabor deconvolution**

A generally accepted model for the seismic trace is to consider it as a convolution of the earth seismic response with a wavelet. In turn, this wavelet can be regarded as the convolution of several effects: source signature, recording filter, earth filter, surface reflections and geophone response (e.g. Robinson, 1980). Deconvolution is the process of removing the wavelet from the seismic trace to estimate the earth seismic response, which is composed of primaries and multiple reflections. The application of deconvolution in seismic processing relies on the fulfillment of a set of assumptions on which the convolutional model is based: stationarity, minimum phase wavelet, and white additive noise.

In the presence of anelastic attenuation, the stationary assumption is not valid. A nonstationary convolutional model (e. g. Margrave et al., 2005) is formulated using the constant-Q theory and the mathematical operation called nonstationary deconvolution (Margrave, 1998).

### *The Constant Q theory*

This is a linear theory in which Q is considered independent of frequency. In the constant Q theory, the propagation of a pulse in an anelastic medium is described by

$$B(f) = \exp\left[-\frac{\pi fx}{V(f_0)Q}\right] \exp\left[\frac{-2\pi ifx}{V(f)}\right], \quad (1)$$

where  $f$  is the frequency,  $V$  is the velocity,  $x$  is the traveled distance and  $Q$  is the attenuation parameter. By using this formula to model the propagation of what initially was a perfect impulse, the effects of attenuation can be observed (Figure 1). In a homogeneous medium the effects can be summarized as: (1) exponential decay with amplitude, due to energy absorption by the medium; (2) broadening of the pulse, due to the fact that higher frequencies are more attenuated; (3) a growing phase delay and (4) an asymmetric pulse shape. The last two effects are due to dispersion, which always accompanies attenuation, according to lab observations, and are relative to nondispersive propagation (velocity independent of frequency). The velocity dispersion relation used in this example is

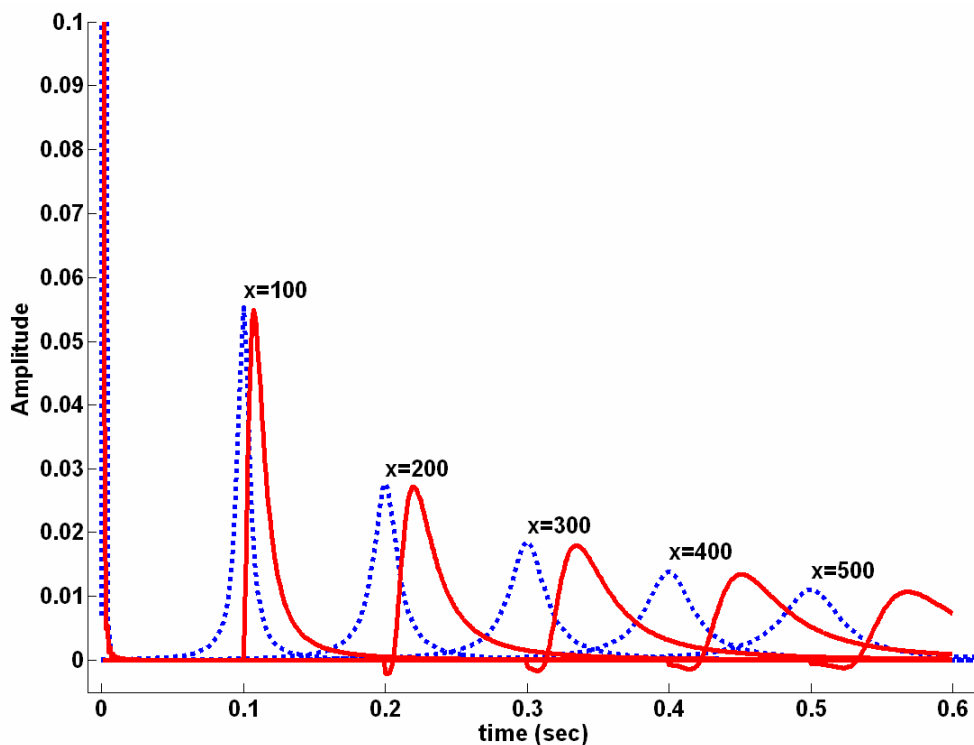


FIG. 1. Propagation of a pulse through a homogeneous anelastic medium. The dotted line corresponds to the case when dispersion is not considered. The continuous line corresponds to the dispersive case.

$$V(f) = V(f_0) \left[ 1 + \frac{1}{\pi Q} \log \left( \frac{f}{f_0} \right) \right], \quad (2)$$

where  $f_0$  is a reference frequency for which the velocity  $V(f_0)$  is known.

*The Nonstationary convolutional model*

The stationary convolutional model can be extended to the nonstationary case by using the operation ‘nonstationary convolution’ as defined by Margrave (1998). This nonstationary model takes into account anelastic attenuation. In the nonstationary convolutional model an attenuated trace  $\hat{\sigma}(f)$  can be modelled as the nonstationary convolution between the attenuation impulse response and the reflectivity, followed by a stationary convolution with the source wavelet as depicted in Figure 2, and as expressed analytically by the time-frequency expression

$$\hat{\sigma}(f) = \hat{w}(f) \int_{-\infty}^{\infty} \alpha_Q(f, \tau) \rho(\tau) e^{-2\pi i f \tau} d\tau, \quad (3)$$

where the hat ( $\hat{\cdot}$ ) symbolizes the Fourier transform,  $w$  is the wavelet,  $\rho$  is the reflectivity,  $\tau$  is the travelttime and  $\alpha_Q(f, \tau)$  is the time-frequency exponential attenuation function, defined as

$$\alpha_Q(f, \tau) = \exp(-\pi f \tau / Q + iH(\pi f \tau / Q)), \quad (4)$$

in which the real and imaginary components in the exponent are connected through the Hilbert transform  $H$ , a result that is consistent with the minimum phase characteristic associated with the attenuation process. As written, equation (3) assumes a spatially constant  $Q$  and models only primaries, though both of these simplifications can be removed with a slight complication in the formula.

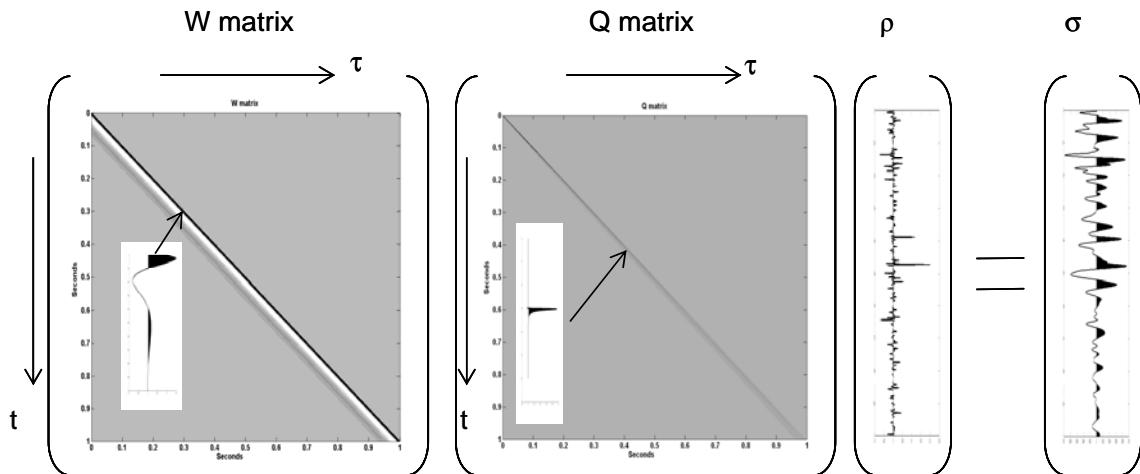


FIG. 2. Nonstationary convolutional model. For the case of finite discrete signals, the stationary and nonstationary convolution operations can be expressed as the multiplication of a matrix by a column vector.

### The Gabor transform

The Gabor transform is a collection of local spectra, a time-frequency representation of a signal obtained with the help of a set of analysis windows. Each local spectrum is obtained by multiplying the signal by a window and taking the Fourier transform of the product. The result constitutes a slice of a time-frequency representation of the signal centred at the midpoint of the window (Figure 3).

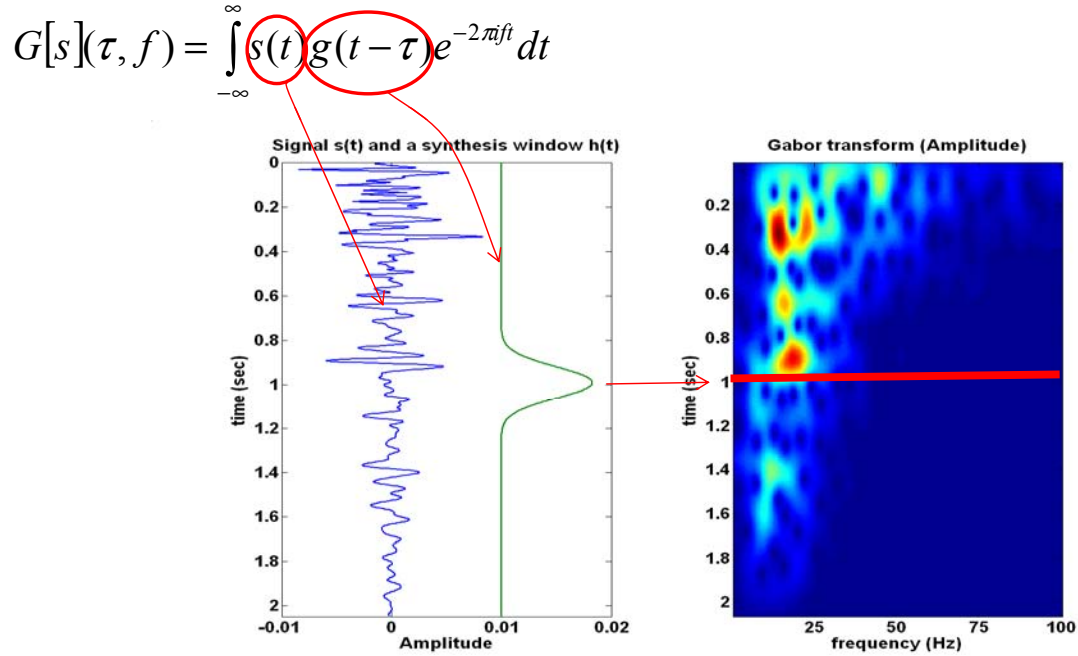


FIG. 3. Generation of the Gabor transform.

Analytically, the Gabor transform,  $G_g[\sigma(t)]$ , of the signal  $\sigma(t)$  is given by

$$G_g[\sigma(t)](\tau, f) = \int_{-\infty}^{\infty} \sigma(t) g(t - \tau) e^{-2\pi jft} dt, \quad (5)$$

where  $g(t)$  is the Gabor analysis window and  $\tau$  is the location of the window center. The subscript  $_g$  emphasizes the fact that different Gabor transforms of the same signal are possible, according to the set of windows chosen.

The inverse Gabor transform is defined as

$$\sigma(t) = \int_{-\infty}^{\infty} \int_{-\infty}^{\infty} G_g[\sigma(t)](\tau, f) \gamma(t - \tau) e^{2\pi jft} df d\tau, \quad (6)$$

where  $\gamma(t)$  is the Gabor synthesis window.  $g(t)$  and  $\gamma(t)$  must satisfy the partition of unity condition

$$\int_{-\infty}^{\infty} g(t)\gamma(t)dt = 1. \quad (7)$$

A highly efficient Discrete Gabor Transform algorithm is obtained by the implementation of a partition of unity based on Lamoureux windows (Grossman et al., 2002).

### The (single channel) Gabor deconvolution algorithm

Gabor deconvolution is a nonstationary extension of Wiener's deconvolution method, based on an approximate, asymptotic factorization of the nonstationary trace model of equation (3), via the Gabor transform,

$$G[\sigma](t, f) \approx \hat{w}(f)\alpha_Q(t, f)G[\rho](t, f), \quad (8)$$

which states that the Gabor transform of the seismic trace,  $G[\sigma](t, f)$ , is approximately equal to the product of the Fourier transform of the source wavelet,  $\hat{w}(f)$ , the time-frequency attenuation function,  $\alpha_Q(t, f)$ , and the Gabor transform of the reflectivity  $G[\rho](t, f)$ .

This factorization is possible thanks to the rich set of mathematical relations that link the Gabor transform and the pseudodifferential operators. Equation (8) is just a first order approximation.

The formulation of Gabor deconvolution from Equation (8) is analogous to the formulation of Wiener deconvolution in the frequency domain. As in Wiener's method, Gabor deconvolution smoothes the Gabor magnitude spectrum of the seismic signal  $|G\sigma(t, f)|$  to estimate  $|\Delta(t, f)|$ , the product of the magnitudes of the attenuation function and the source signature,

$$|\Delta(t, f)| \approx |\hat{w}(f)| |\alpha_Q(t, f)|. \quad (9)$$

A phase function for  $\Delta(t, f)$  is then estimated, with the help of the digital Hilbert transform,  $H$ , using the minimum phase assumption,

$$\varphi(t, f) = H(\ln|\Delta(t, f)|). \quad (10)$$

Finally the Gabor spectrum of the reflectivity is estimated in the Gabor domain as:

$$G[\rho](t, f)_{est} = \frac{G\sigma(t, f)}{\Delta(t, f)}, \quad (11)$$

and the reflectivity estimate is then recovered as the inverse Gabor transform of the result of equation (11). Removal of the source signature and compensation for attenuation are applied simultaneously in this process. The algorithm is sketched in Figure 4.

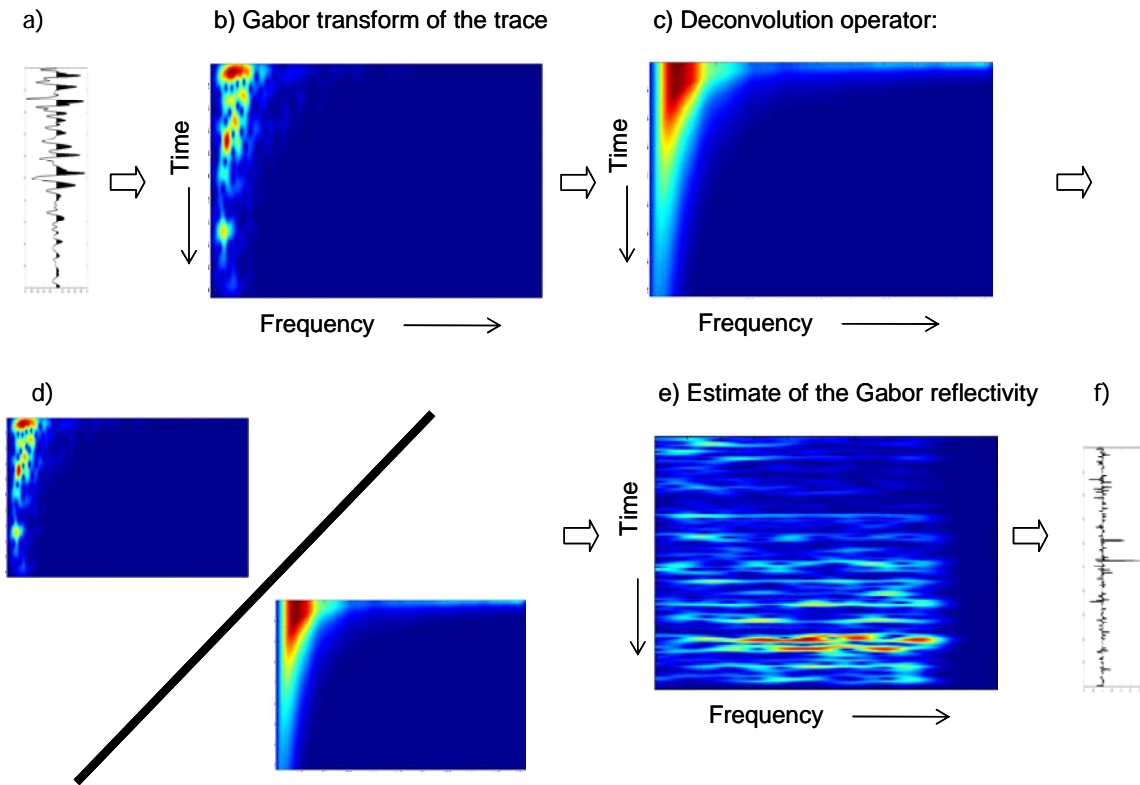


FIG. 4. Sketch of the single channel Gabor deconvolution algorithm. The first step is to compute the Gabor transform, (b), of the attenuated trace, (a). Then the deconvolution operator, (c), is built by smoothing (b) and computing its minimum phase through the Hilbert transform. Finally, by spectrally dividing (b) by (c), an estimate of the Gabor transform, (e), of the deconvolved trace, (f), is obtained.

### Smoothing

A very important element of the Gabor algorithm is the smoothing process. Different kinds of smoothing are possible, Iliescu and Margrave (2002) use 2D boxcar smoothing and hyperbolic smoothing along curves of  $\tau f = \text{constant}$ . For the surface-consistent implementation of Gabor deconvolution presented below, the hyperbolic smoothing method is used, because it allows explicit estimations of the wavelet  $\hat{w}(f)$  and the amplitude of the attenuation function,  $|\alpha_Q(\tau, f)|$ . Grossman et al. (2002) use a different method to estimate  $|\hat{w}(f)|$  and  $|\alpha_Q(\tau, f)|$  based on least square fitting of equation (8), which also produces an estimate of Q.

### Minimum phase

Minimum phase is an essential concept in Gabor deconvolution. Besides the minimum-phase character associated with the source wavelet generated by an explosive source, the constant-Q theory gives strong arguments to assert that the attenuation earth filter is also endowed with a minimum-phase character (e.g. Futterman, 1962).

In signal theory a minimum phase wavelet is defined as a causal stable wavelet with a causal stable inverse, in which the term ‘stable’ is associated with a precise physical

meaning: finite energy. A minimum phase wavelet is also the one on which energy arrives the earliest among all possible causal, invertible wavelets with the same amplitude spectrum.

For this special kind of wavelet, the mathematical theory gives an extraordinary, interesting and useful result: the phase spectrum of a minimum phase wavelet is equal to the Hilbert transform of the logarithm of its amplitude spectrum.

### Hilbert transform

The estimation of the phase spectrum of the Gabor deconvolution operator is achieved by resorting to the minimum phase assumption via the Hilbert transform. The Hilbert transform of the deconvolution operator is found either analytically, by using the equation

$$\varphi_A(f) = H[\alpha(f)] = \frac{f}{V(f)} - \frac{f}{V_\infty}, \quad (12)$$

which is a mathematical result from the linear casual constant Q theory for attenuation (Futterman, 1962), or digitally, by using the mathematical definition of the Hilbert transform,

$$\varphi_D(f) = \int_{-\infty}^{\infty} \frac{\ln|\Delta(f')|}{f - f'} df' \approx \sum_{f'=-Nyq}^{Nyq} \frac{\ln|\Delta(f')|}{f - f'} \delta f'. \quad (13)$$

Although the equation (12) is an analytical expression for computing the phase, it has the inconvenience that it depends on the phase velocity, given by Equation (2), which in turn depends explicitly on the attenuation parameter Q. This explicit dependence on Q makes this method for computing the Hilbert transform only suitable for the cases when a good estimation of Q is available. Unfortunately, in the majority of the practical cases, the uncertainty associated with Q is high, and this uncertainty is transmitted to the phase computed in this way. The digital method to compute phase, using Equation (13), has the advantage of not being explicitly dependent on Q; therefore the estimation of Q is data driven. However there are two disadvantages associated with this digital estimation: an error in the estimation of the integral, and high sensitivity to noise. An error in the phase is generated by the substitution of the infinite limits in the definition of the Hilbert transform by finite limits determined by the sample rate (Equation 13). An approximate solution to this problem, adding a correction term linear in time and quadratic in frequency, is presented and discussed in Montaña and Margrave (2005).

An important issue in the consideration of the digital Hilbert is the impact of noise. In Figures 5 to 7, an experiment is shown in which noisy versions of a synthetic attenuated trace, with different signal to noise ratio (S/N), were Gabor deconvolved. The input traces are shown in Figure 5, the output traces in Figure 6 and a plot of the local cross-correlation between the real and the expected output as a function of time and S/N is shown in Figure 7. The local cross-correlation is obtained by taking the cross-correlation between the two traces inside short windows, and extracting the maximum coefficient of the cross-correlation as a local attribute to quantify the quality of the result.

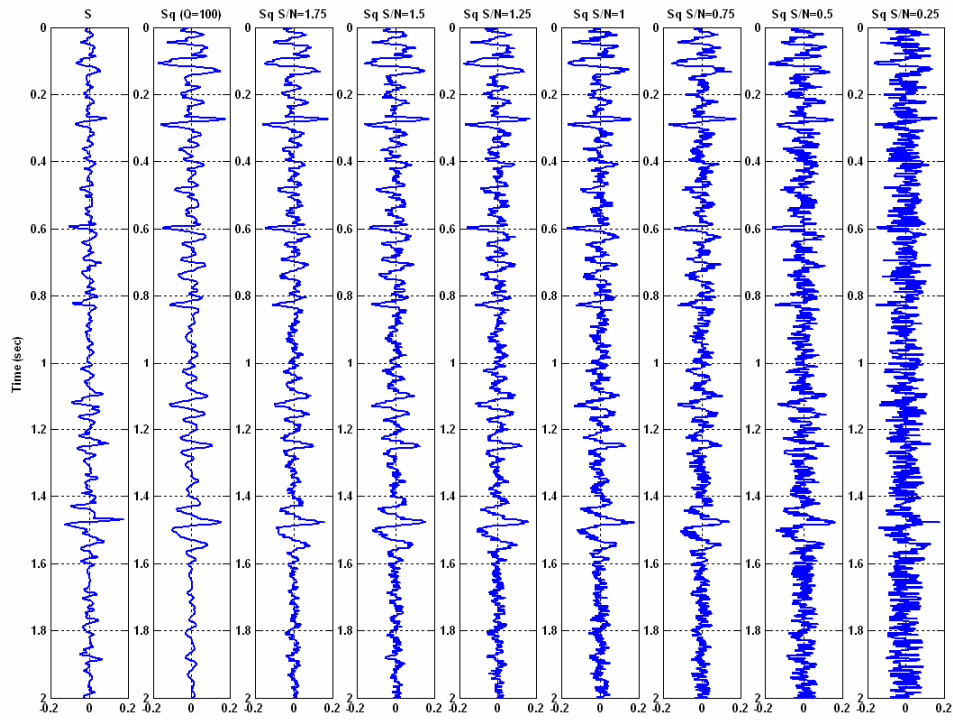


FIG. 5. A seismic trace (S), its attenuated version (Sq) for Q=100, and five noisy versions of Sq for different signal to noise ratios.

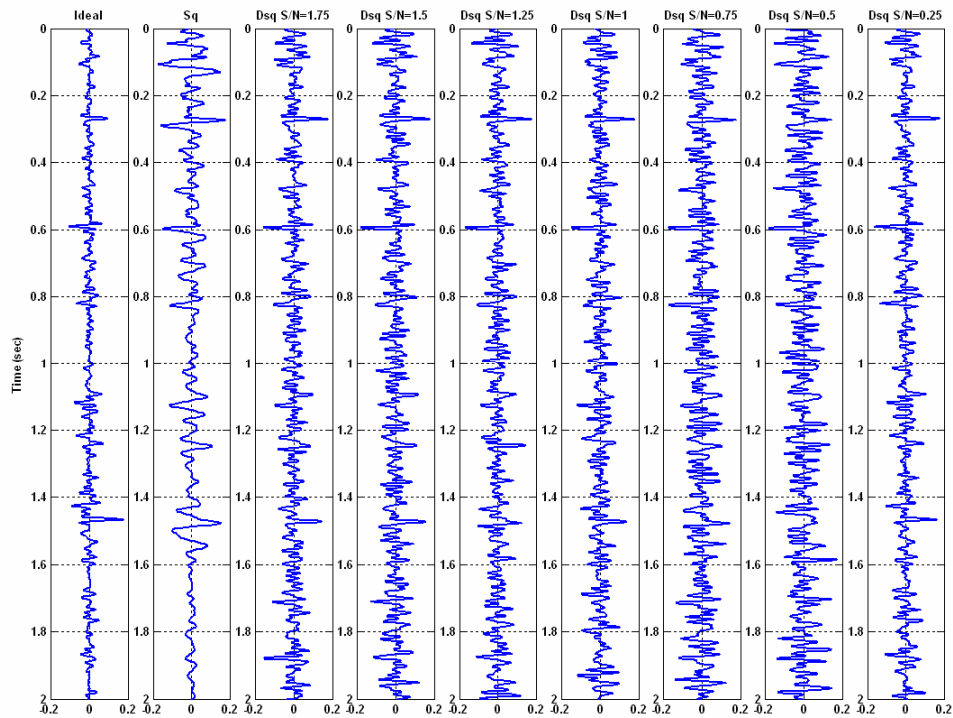


FIG. 6. The ideal output, the clean input (Sq) and the output for the Gabor deconvolution of the traces shown in the previous figure. Each trace is identified by its S/N. All the outputs were filtered to a maximum frequency of 70 Hz.

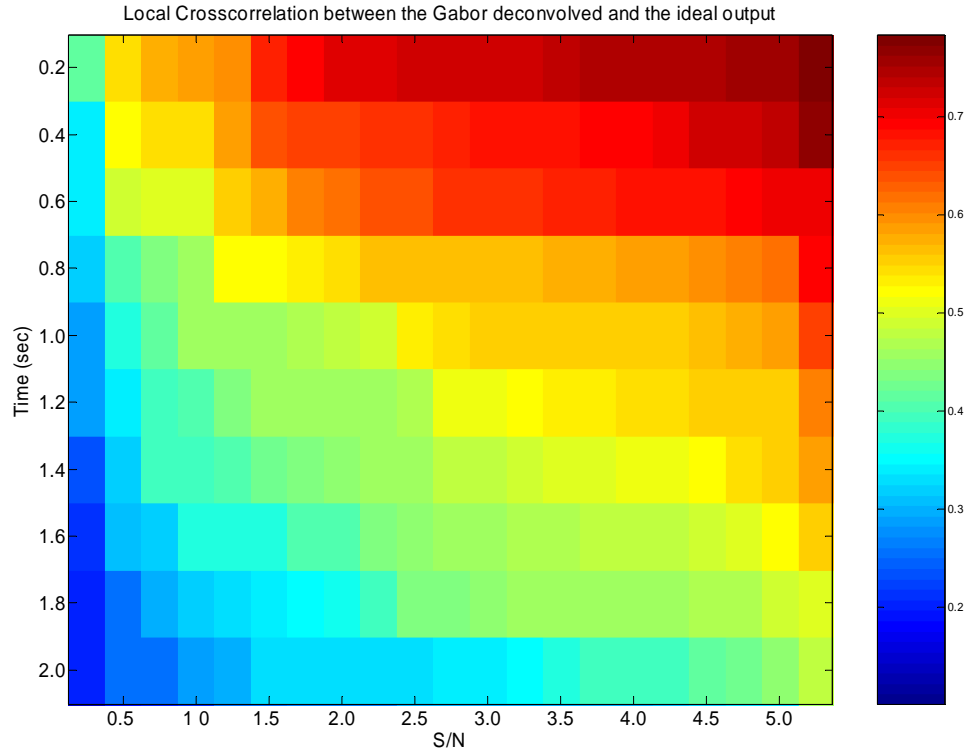


FIG. 7. Local cross-correlation between the Gabor deconvolved traces for different S/N and the ideal output. The deterioration of the quality of the output grows with lower S/N and also with time.

It can be observed how the results deteriorate when the S/N ratio increases and/or when the time increases. This experiment shows the harmful effects of noise on the performance of minimum phase Gabor deconvolution, effects that need to be minimized to improve the quality of the results.

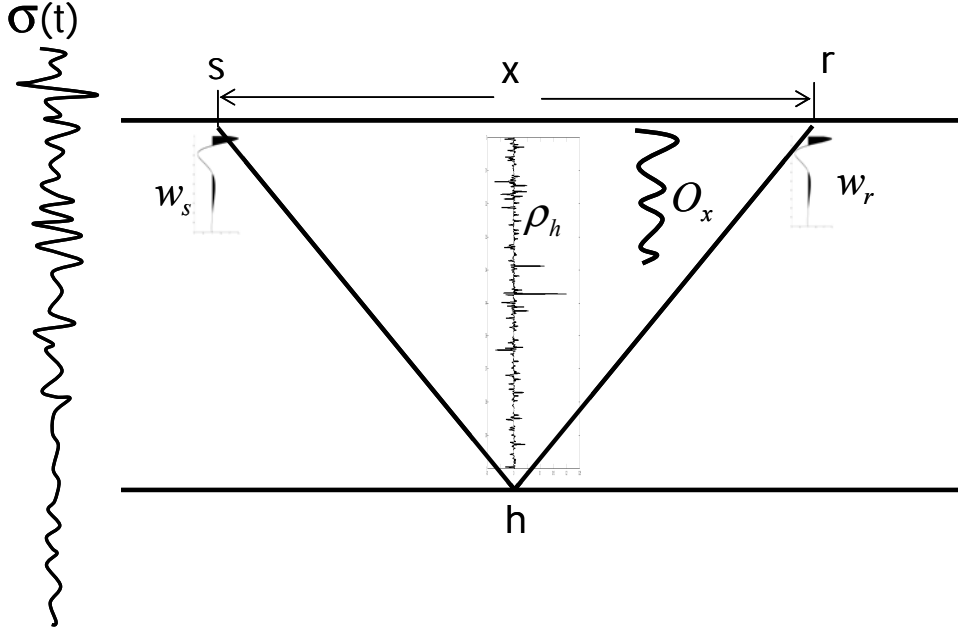
### The surface-consistent convolutional model

In this model the earth's effects on a seismogram are classified into those caused by the near surface and those caused by the subsurface. In practice the near surface effects are associated with the source and the receiver coordinates, whereas subsurface effects are those which vary as a function of midpoint and offset (Figure 8).

The surface consistency concept can be applied to the nonstationary convolutional model for the seismic trace, stated above in equation (8), by introducing two modifications. The first modification is to split the wavelet appearing in the original single channel formulation into two wavelets: a source wavelet component that depends on the source coordinate, and a receiver wavelet component that depends exclusively on the receiver coordinate. The second modification is the assignment of an exclusive dependence on the midpoint coordinate to the attenuation and reflectivity factors (Figure 9). With these modifications the surface-consistent nonstationary convolutional model is expressed by

$$G[\sigma](f, \tau, h, r, s) = [w_s(f, s)] \alpha_\rho(f, \tau, h) [G[\rho](f, \tau, h)] [w_r(f, r)] \quad (14)$$

where  $s$ ,  $r$  and  $h$  are the source, receiver and midpoint coordinates respectively,  $G[\sigma](f, \tau, h, r, s)$  is the Gabor transform of the surface-consistent seismic trace,  $w_s(f, s)$  and



$$\sigma(s, r, x, h, t) = w_s(s, t) \otimes \rho_h(h, t) \otimes O_x(x, t) \otimes w_r(r, t)$$

FIG. 8. Surface-consistent convolutional model for the seismic trace. In this model the trace is considered as the convolution of 4 components: source wavelet, receiver wavelet, midpoint and offset components.

$w_r(f, r)$  are the Fourier transform of the source and receiver wavelets respectively (including the near surface attenuation effects),  $\alpha(f, \tau, h)$  represents the subsurface attenuation effects and  $G[\rho](f, \tau, h)$  is the Gabor transform of the reflectivity.

### A first approach to a surface-consistent Gabor deconvolution algorithm

For the description of the algorithm each trace will be identified by a set of indices  $i, j, k$  corresponding to the midpoint, source and receiver locations respectively. The algorithm is sketched in Figures 9 and 10 and can be summarized as follows. The single-channel Gabor deconvolution algorithm, using hyperbolic smoothing, is applied to each trace. The output of this step on the  $\sigma_{ijk}(t)$  trace are estimations of the amplitude component of the  $i^{\text{th}}$  midpoint subsurface attenuation operator,  $|\alpha(\omega, \tau, x_i)|$  and the wavelet  $w_{jk}$ . The  $j^{\text{th}}$  source wavelet,  $w_s(\omega, s_j)$ , and the  $k^{\text{th}}$  receiver wavelet,  $w_r(\omega, r_k)$  are estimated as the square root of the wavelet  $w_{jk}$ . The estimated components are stored in midpoint, source and receiver arrays, in the bin corresponding to the indices of the trace (Figure 9).

The next step is to do ensemble averages in the source receiver and midpoint domain (Figure 10). The components stored in each bin are stacked, and then the stacks combined

to create the magnitude of the surface-consistent Gabor deconvolution operator,  $|\theta_{ijk}(\omega, \tau)|$ , for the trace  $\sigma_{ijk}(t)$ ,

$$|\theta_{ijk}(f, \tau)| = A_i ** (w_s)_j \cdot (w_r)_k, \quad (15)$$

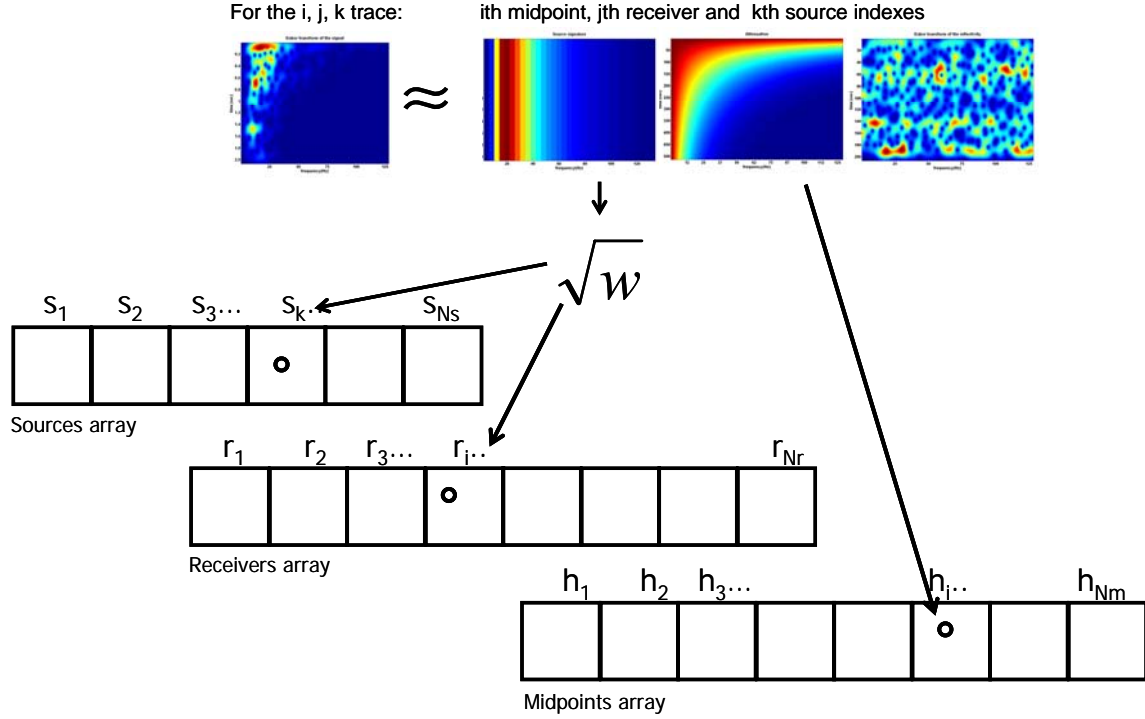


FIG. 9. Surface-consistent Gabor deconvolution. From the single channel Gabor deconvolution, the source, receiver and midpoint components of each trace are stored in arrays.

where  $(**)$  denotes element by element multiplication between a column vector and the rows of a matrix,  $(\cdot)$  means element by element matrix multiplication, and the matrix  $A_i$  and the vectors  $(w_s)_j$  and  $(w_r)_k$  are defined by,

$$A_i = \frac{\sum_{l=1}^{L_i} |\alpha(f, \tau, x_l)|_i}{L_i}, \quad (15a)$$

$$[w_s]_j = \frac{\sum_{m=1}^{M_j} |w_s(f, s_m)|_j}{M_j}, \quad (15b)$$

$$[w_r]_k = \frac{\sum_{n=1}^{N_k} |w_r(f, r_n)|_k}{N_k}, \quad (15c)$$

where  $L_i$ ,  $M_j$  and  $N_k$  are the CMP, source and receiver folds respectively.

As it is assumed that  $\theta_{ijk}(f, \tau)$  is a minimum-phase function, its phase component is estimated from its amplitude spectrum using the Hilbert transform as

$$\varphi_{ijk}(f, \tau) = \int_B \frac{\ln|\theta_{ijk}(f', \tau)|}{f - f'} df', \quad (16)$$

where  $B$  denotes the available spectral band. It is not hard to see why the computation of phase through equation (16) could be harmed by the presence of noise. For any frequency, the phase is found as an integral over all the frequencies, thus the presence of noise at a particular frequency will affect the phase at any other frequency.

Finally the Gabor spectrum of the reflectivity,  $G\rho_{ijk}(f, \tau)_{est}$  is estimated in the Gabor domain as

$$Gr_{ijk}(f, \tau)_{est} = \frac{G\sigma_{ijk}(f, \tau)}{\theta_{ijk}(f, \tau)}, \quad (17)$$

where  $G\sigma_{ijk}(f, \tau)$  is the Gabor transform of the seismic trace.

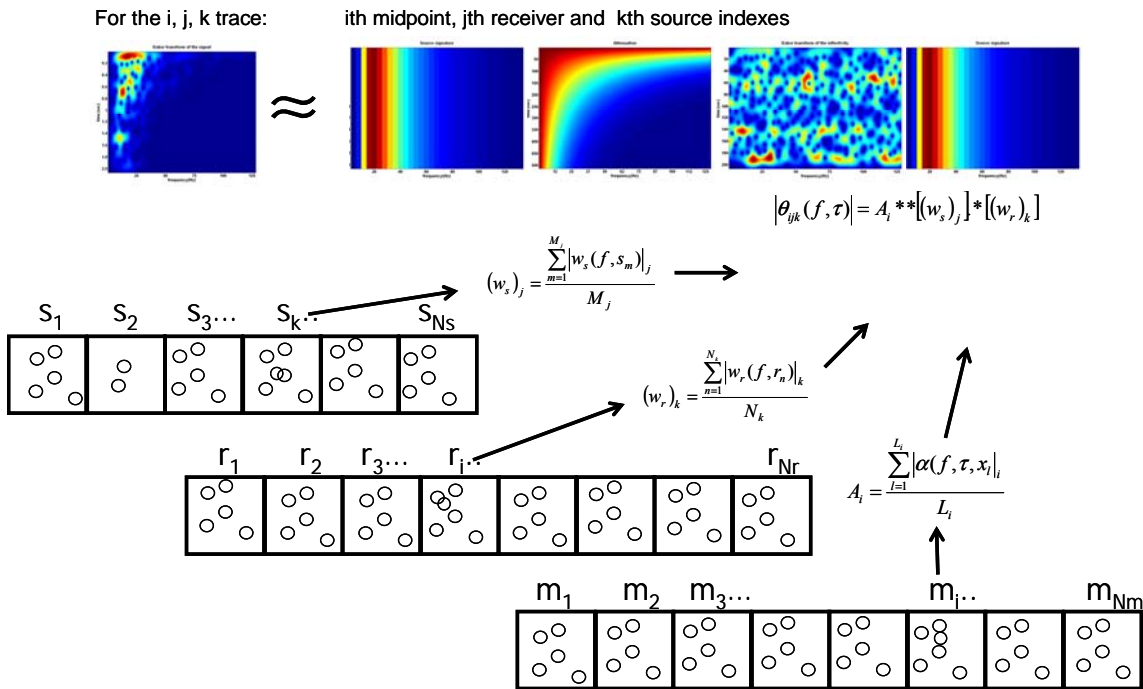


FIG. 10. The surface-consistent deconvolution operator is built by combining the ensemble average in the source, receiver and midpoint domain of the components computed in the single-channel Gabor deconvolution process.

### EXAMPLES

For the first example a synthetic dataset (courtesy of DIVESTCO) is used to test the method. This dataset is really challenging for any surface consistent, and/or attenuation compensation method due to the combination of three elements in its generation: strong

attenuation, convolution with surface-consistent source and receiver-wavelets and strong random noise. It was generated using the reflectivity series from a real well log, storing the reflectivity into the zeroed traces of a real seismic line, applying forward NMO and forward Q filtering with  $Q=40$ , and then convolving each trace with surface-consistent minimum phase source and receiver wavelets. Finally random noise, with strength varying from trace to trace in such a way as to mimic acquisition on a windy day, was added to each trace. The dataset is made up of 78 shots, 96 channels per shot, 2 seconds length. Its generation is sketched in Figure 11. Signal to noise ratio analysis of one typical shot and a brute stack are shown in figure 12. A detailed signal analysis of this dataset is presented by Henley et al. (2006) in a different paper of this report.

After the application of minimum phase, single-channel Gabor deconvolution to the raw shots (Figure 13), the computation of the phase through equation (13) is dramatically distorted in the areas with low S/N, especially the original flat reflectors between 1300 and 1600 ms have been transformed into fake complex structures.

After the application of minimum phase, single-channel Gabor deconvolution to the raw shots (Figure 4), the computation of the phase through equation (4) is dramatically distorted. The stack of the deconvolved data is shown in Figure 5, clearly showing how the original flat reflectors between 1300 and 1600 ms have been transformed into fake complex structures.

The application of the minimum phase, surface-consistent Gabor deconvolution to the raw shots is much less sensitive to the presence of noise as can be seen in the stack of the deconvolved shots shown in Figure 7. The reflectors between 1300 and 1600 ms do not show the fake complexity introduced by the single-channel Gabor deconvolution.

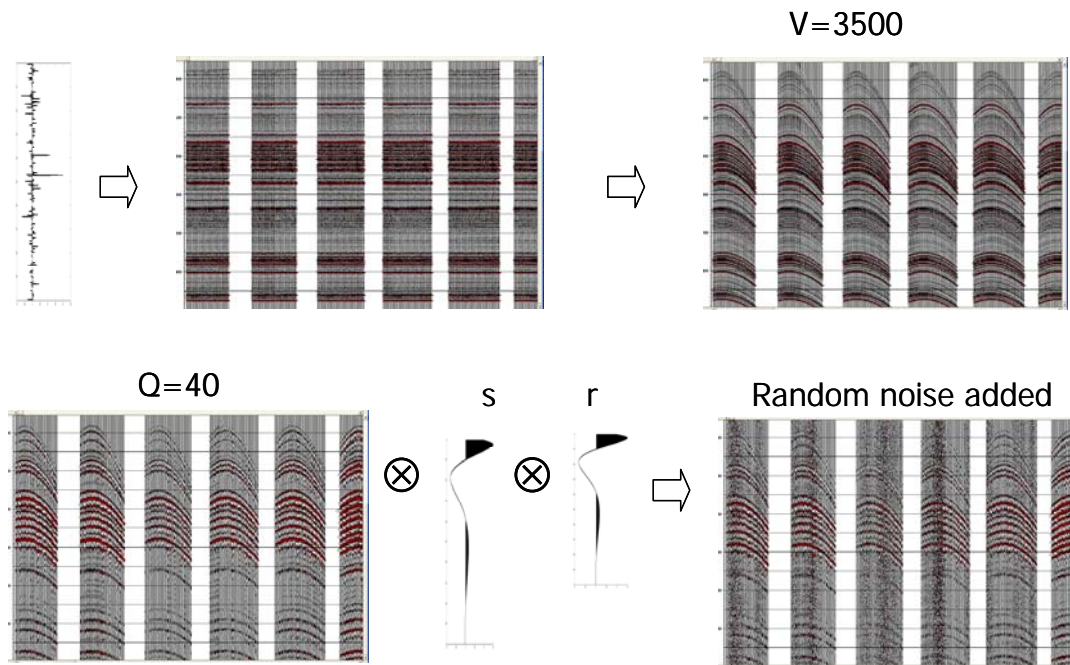


FIG. 11. Generation of the synthetic dataset used to test the surface-consistent Gabor deconvolution algorithm.

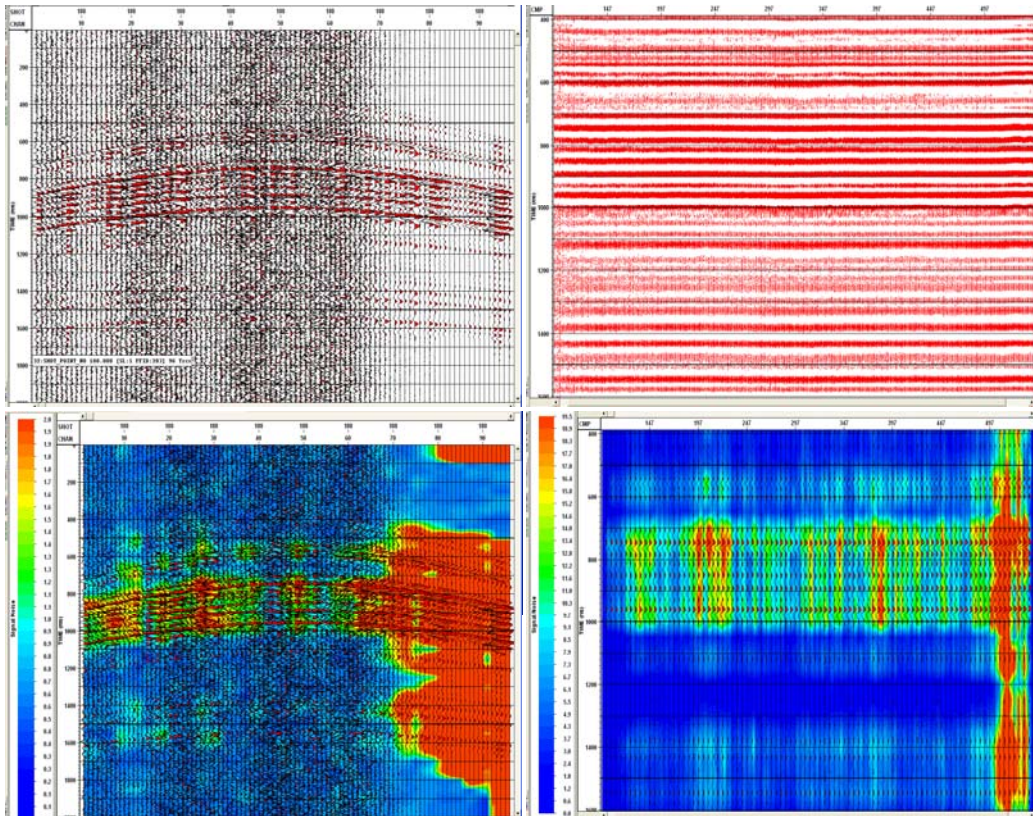


FIG. 12. The bottom panels show the signal to noise ratio analysis of the synthetic data shown in the top panels. To the left is shown the S/N analysis of one shot, and to the right the corresponding S/N of the brute stack. Only the red areas have good S/N. In the green the S/N is acceptable and the bluish is poor.

## CONCLUSIONS

A poor signal to noise ratio may harm the estimation of the minimum phase Gabor deconvolution operator, introducing undesirable artifacts into the results. The Surface-Consistent implementation of Gabor deconvolution allows a robust estimation of the minimum phase deconvolution operator with respect to random noise and surface-consistent variations in the source and receiver wavelets.

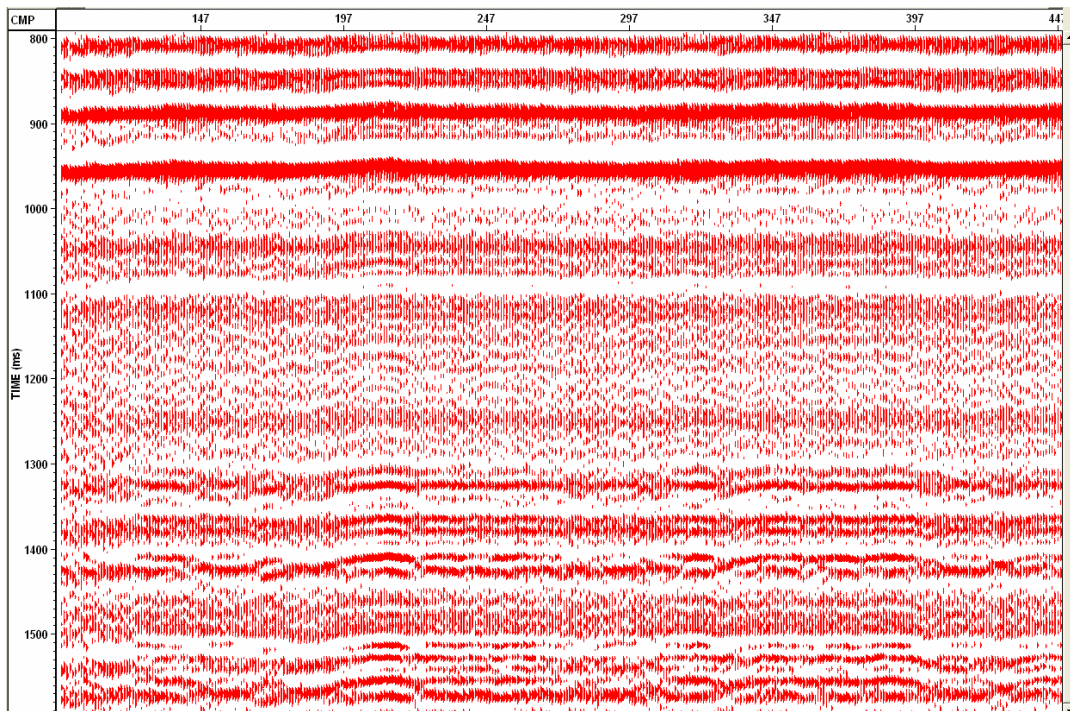


FIG. 13. Stack of the synthetic data shown in figures 10 to 12, after prestack single channel Gabor deconvolution was applied. The distortions introduced by noise into the computation of the Hilbert transform are evident in the reflectors between 1300 and 1600 ms.

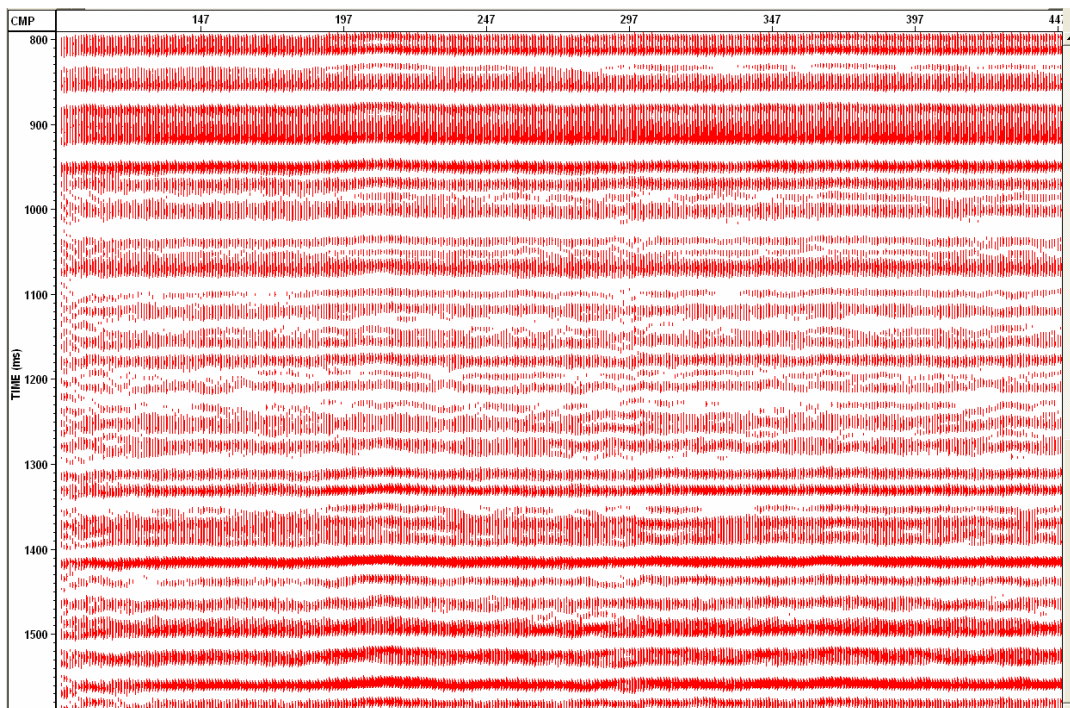


FIG. 14. The same data shown in the previous figure, but surface-consistent instead of single channel Gabor deconvolution was used. The negative effects of noise on the computation of the Hilbert transform has been strongly attenuated by the surface consistent estimation of the Gabor deconvolution operator.

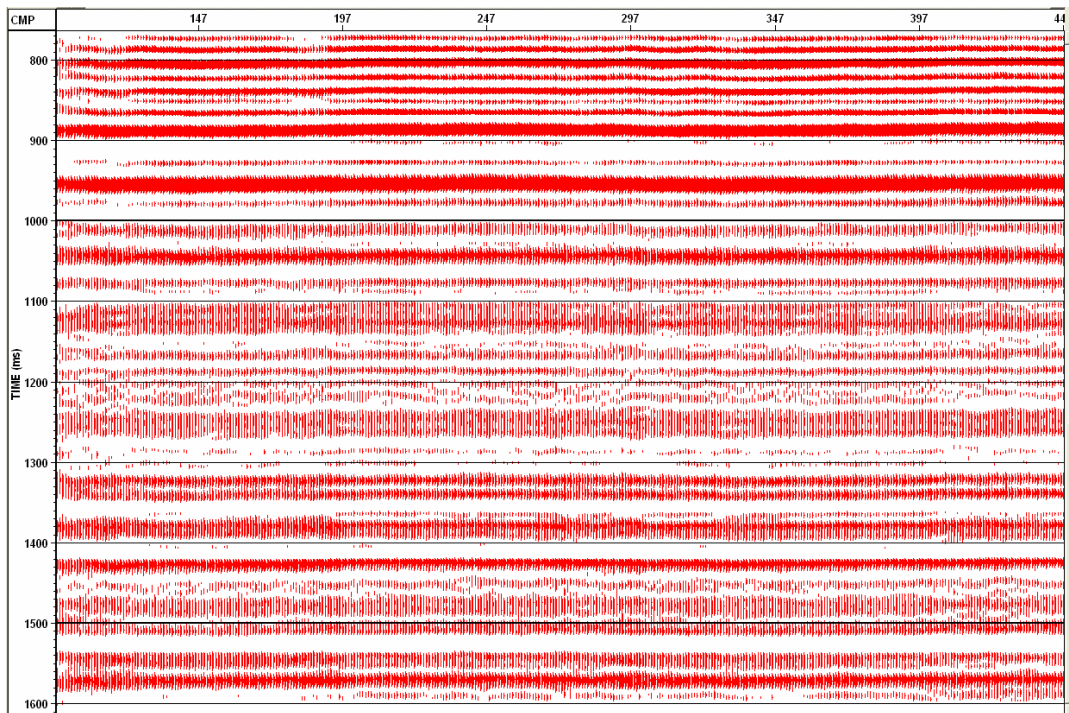


FIG. 15. Same data of the previous 2 figures but instead of Gabor deconvolution, the conventional flow process (surface consistent Wiener deconvolution combined with TVSW) was used.

### ACKNOWLEDGEMENTS

The authors would like to thank Keith Hirsche from Hampson and Russell for his helpful comments regarding phase and Hilbert transform, and the sponsors of the CREWES Project, the Canadian government funding agencies, NSERC, and MITACS, the CSEG and the Department of Geology and Geophysics University of Calgary for their financial support to this project.

### REFERENCES

- Aki, K., and Richards, P. G., 2002, *Quantitative Seismology: Theory and methods*. University Science Books.
- Dasgupta, R., and Clark, R. A., 1999, Estimation of  $Q$  from seismic surface reflected data: *Geophysics*, **63**, 2120-2128
- Duren, R. E., and Trantham, E. C., 1997, Sensitivity of the dispersion correction to  $Q$  error: *Geophysics*, **62**, 288-290.
- Gabor, D., 1946, Theory of communication: *J. Inst. Electr. Eng.*, **93**, 429-457.
- Grossman, J. P., Margrave G. F., Lamoureux M. P., and Aggarwala, R., 2002, Constant- $Q$  wavelet estimation via a Gabor spectral model: *CSEG Convention Expanded Abstracts*.
- Grossman, J. P., Margrave G. F., and Lamoureux M. P., 2002, Constructing nonuniform Gabor frames from partition of unity. *CREWES Research Report*, **14**
- Kjartansson, E., 1979, Constant- $Q$  wave propagation and attenuation: *J. Geophysics. Res.*, **84**, 4737-4748
- Hale, D., 1981, An Inverse- $Q$  filter: *SEP Report* **26**.
- Henley, D.C, Montana, C, and Margrave, G., 2006, Ensemble-based deconvolution: when and why, *CREWES Research Report*, **17**.
- Iliescu, V., and Margrave G. F., 2002, Reflectivity amplitude restoration in Gabor deconvolution: *CSEG Convention Expanded Abstracts*.

- Iliescu, V., 2002, Seismic signal enhancement using time-frequency transforms. Thesis M.Sc. University of Calgary,
- Margrave, G. F., 1998, Theory of nonstationary linear filtering in the Fourier domain with application to time-variant filtering: *Geophysics*, **63**, 244-259.
- Margrave, G. F., and Lamoureux M. P. 2002, Gabor deconvolution: 2002 CSEG Annual Convention, Calgary, AB.
- Margrave G. F., Dong, L. Gibson, P., Grossman, J. P., Henley D., and Lamoureux M. P., 2003, Gabor Deconvolution: Extending Wiener's Method to nonstationarity: CREWES Research Report, **15**.
- Mertins, A., 1999, *Signal Analysis*: John Wiley and Sons.
- Montana C. A., and Margrave G. F., 2004, Compensating for attenuation by inverse- $Q$  filtering, CREWES Research Report, **16**.
- Robinson, E. A. and Treitel, S., 1980, *Geophysical Signal Analysis*, Prentice-Hall.
- Schoepp, A. R., and Margrave, G. F., 1998, Improving seismic resolution with nonstationary deconvolution: 68<sup>th</sup> Annual SEG meeting.
- Schoepp, A. R., 1998, Improving seismic resolution with nonstationary deconvolution. Thesis M.Sc. University of Calgary
- Wang, Y., 2002, An stable and efficient approach of inverse- $Q$  filtering: *Geophysics*, **67**, 657-663.